J|A|C|S
ARTICLES
Published on Web 07/24/2004

Photoisomerization Dynamics of Azobenzene in Solution with S_1 Excitation: A Femtosecond Fluorescence Anisotropy Study

Chih-Wei Chang, Ying-Chih Lu, Tsai-Te Wang, and Eric Wei-Guang Diau*

Contribution from the Department of Applied Chemistry and Center for Interdisciplinary Molecular Science, National Chiao Tung University, Hsinchu, Taiwan 30050

Received February 12, 2004; E-mail: diau@mail.ac.nctu.edu.tw

Abstract: Measurements of anisotropy of femtosecond fluorescence after direct excitation of the $S_1(n,\pi^*)$ state of azobenzene in hexane and ethylene glycol solutions have been carried out to address the controversy about inversion and rotation in the mechanism of photoisomerization. The observed anisotropies in hexane decay to a nonzero asymptotic level with a relaxation period the same as that for slow decay of the corresponding biexponential transient; this effect is attributed to involvement of the out-of-plane CNNC-torsional motion on approach to a twisted conical intersection along the "rotation channel" that depolarizes the original in-plane transition moment. In contrast, when the rotational channel becomes substantially hindered in ethylene glycol, the anisotropies show no discernible decay feature, but the corresponding transients show prominent decays attributed to involvement of in-plane symmetric motions; the latter approach a planar-sloped conical intersection along a "concerted inversion channel" for efficient internal conversion through vibronic coupling. The proposed mechanism is consistent with theoretical calculations and rationalizes both results on quantum yields and ultrafast observations.

1. Introduction

The photoisomerization of azobenzene and its derivatives has attracted interest because of its potential applications in optical switching and memory storage,[1−4] biochemical activity,[5,6] molecular machines,[7] and nanodevices.[8] Photoexcitation of *trans*-azobenzene (AB) into electronically excited states leads to isomerization, and both trans and cis isomers are produced in the ground state.[9] The mechanism of photoisomerization of AB has been controversial for almost two decades,[9−15] therefore prompting many experimental[16−24] and theoretical[14,15,24−29] investigations.

UV−visible spectra of AB in solutions in the steady state exhibit two absorption features assigned to $S_0 \rightarrow S_1$ and $S_0 \rightarrow S_2$ transitions.[9] In the visible region, the $S_0 \rightarrow S_1$ transition with maximum intensity near 450 nm is interpreted as involving perpendicular excitation of an electron from the nonbonding *n* orbital of an N atom to an antibonding π^* orbital. For a molecule with symmetry according to point group C_{2h}, this electronic transition $-\tilde{A}^1B_g \leftarrow \tilde{X}^1A_g -$ is forbidden.[9] In the UV region, the $S_0 \rightarrow S_2$ transition with maximum intensity near 320 nm is associated with a symmetry-allowed $\pi-\pi^*$ transition. The features of the latter transition of AB resemble those of stilbene,[30] possessing a central CC double bond for its $\pi-\pi^*$ transition.

(1) Kumar, G. S.; Neckers, D. C. *Chem. Rev.* **1989**, *89*, 1915−1925.
(2) Liu, Z. F.; Hashimoto, K.; Hujishima, A. *Nature* **1990**, *347*, 658−660.
(3) Ikeda, T.; Tsutsumi, O. *Science* **1995**, *168*, 1873−1875.
(4) Berg, R. H.; Hvilsted, S.; Ramanujam, P. S. *Nature* **1996**, *383*, 505−508.
(5) Willner, I.; Rubin, S.; Riklin, A. *J. Am. Chem. Soc.* **1991**, *113*, 3321−3325.
(6) Ulysse, L.; Cubillos, J.; Chmielewski, J. *J. Am. Chem. Soc.* **1995**, *117*, 8466−8467.
(7) Harada, A. *Acc. Chem. Res.* **2001**, *34*, 456−464.
(8) Banerjee, I. A.; Yi, L.; Matsui, H. *J. Am. Chem. Soc.* **2003**, *125*, 9542−9543.
(9) Rau, H. In *Photochromism: Molecules and Systems*; Durr, H., Bouas-Laurent, H., Eds.; Elsevier: Amsterdam, 1990, pp 165−192 and references therein.
(10) Rau, H.; Lüddecke, E. *J. Am. Chem. Soc.* **1982**, *104*, 1616−1620.
(11) Biswas, N.; Umapathy, S. *Chem. Phys. Lett.* **1995**, *236*, 24−29.
(12) Tamai, N.; Miyasaka, H. *Chem. Rev.* **2000**, *100*, 1875−1890.
(13) Fujino, T.; Arzhantsev, S. Y.; Tahara, T. *Bull. Chem. Soc. Jpn.* **2002**, *75*, 1031−1040.
(14) Ciminelli, C.; Granucci, G.; Persico, M. *Chem.−Eur. J.* **2004**, *10*, 2327−2341.
(15) Diau, E. W.-G. *J. Phys. Chem. A* **2004**, *108*, 950−956.
(16) Lednev, I. K.; Ye, T.-Q.; Hester, R. E.; Moore, J. N. *J. Phys. Chem.* **1996**, *100*, 13338−13341.
(17) Nägele, T.; Hoche, R.; Zinth, W.; Wachtveitl, J. *Chem. Phys. Lett.* **1997**, *272*, 489−495.
(18) Lednev, I. K.; Ye, T.-Q.; Matousek, P.; Towrie, M.; Foggi, P.; Neuwahl, F. V. R.; Umapathy, S.; Hester, R. E.; Moore, J. N. *Chem. Phys. Lett.* **1998**, *290*, 68−74.
(19) Lednev, I. K.; Ye, T.-Q.; Abbott, L. C.; Hester, R. E.; Moore, J. N. *J. Phys. Chem. A* **1998**, *102*, 9161−9166.
(20) Fujino, T.; Tahara, T. *J. Phys. Chem. A* **2000**, *104*, 4203−4210.
(21) Fujino, T.; Arzhantsev, S. Y.; Tahara, T. *J. Phys. Chem. A* **2001**, *105*, 8123−8129.
(22) Lu, Y.-C.; Chang, C.-W.; Diau, E. W.-G. *J. Chin. Chem. Soc.* **2002**, *49*, 693−701.
(23) Schultz, T.; Quenneville, J.; Levine, B.; Toniolo, A.; Martinez, T. J.; Lochbrunner, S.; Schmitt, M.; Shaffer, J. P.; Zgierski, M. Z.; Stolow, A. *J. Am. Chem. Soc.* **2003**, *125*, 8098−8099.
(24) Satzger, H.; Sporlein, S.; Root, C.; Wachtveitl, J.; Zinth, W.; Gilch, P. *Chem. Phys. Lett.* **2003**, *372*, 216−223.
(25) Cattaneo, P.; Persico, M. *Phys. Chem. Chem. Phys.* **1999**, *1*, 4739−4743.
(26) Ishikawa, T.; Noro, T.; Shoda, T. *J. Chem. Phys.* **2001**, *115*, 7503−7512.
(27) Fliegl, H.; Kohn, A.; Hattig, C.; Ahlrichs, R. *J. Am. Chem. Soc.* **2003**, *125*, 9821−9827.
(28) Ikegami, T.; Kurita, N.; Sekino, H.; Ishikawa, Y. *J. Phys. Chem. A* **2003**, *107*, 4555−4562.
(29) Cembran, A.; Bernardi, F.; Garavelli, M.; Gagliardi, L.; Orlandi, G. *J. Am. Chem. Soc.* **2004**, *126*, 3234−3243.
(30) Waldeck, D. H. *Chem. Rev.* **1991**, *91*, 415−436 and references therein.

Scheme 1. The Conventional Inversion versus Rotation Mechanisms

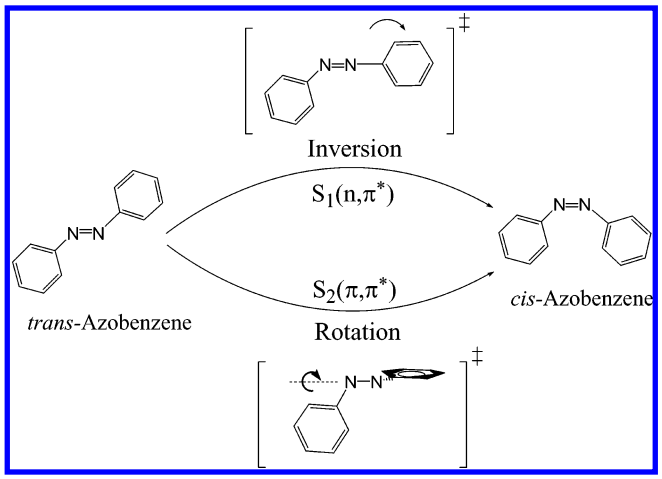

Measurements[31,32] in the steady state show that quantum yields (ϕ) for trans → cis photoisomerization through the $S_0 \rightarrow S_1$ and $S_0 \rightarrow S_2$ transitions differ: in hexane, $\phi = 0.20-0.27$ and $0.09-0.12$, respectively; distinct isomerization mechanisms might therefore operate after excitations into separate electronically excited states.[9] Results of Rau and Lüddecke,[10] Rau,[33] and Bortolus and Monti[34] show almost the same ϕ values for AB and its derivatives in which rotation about the NN double bond is restricted. Two mechanisms of photoisomerization have been proposed:[9,12] excitation to the $S_1(n,\pi^*)$ state might implement isomerization via inversion about one nitrogen atom in the same molecular plane, whereas excitation to the $S_2(\pi,\pi^*)$ state might produce isomerization via rotation about the NN double bond (Scheme 1). Calculations of molecular electronic structure by Monti et al.[35] support this interpretation that has been widely adopted in research on AB[17−19] and its derivatives[12,19,36,37] using time-resolved femtosecond (fs) transient absorption spectroscopy.

This dual mechanism was challenged by Tahara and coworkers,[13,20,21] whose insightful work was based on time-resolved measurements with abundant dynamical and spectral information. Fujino and Tahara[13,20] reported that the wavenumber of the NN-stretching mode observed in picosecond (ps) transient Raman spectra of AB, upon excitation to the S_2 state at the excitation wavelength (λ_{ex}) 273 nm, is near that of the ground state: 1428 cm^{-1} vs 1440 cm^{-1}. The observed transient Raman spectra were assigned to the S_1 species; the lifetime of this transient state was reported to depend strongly on solvent: ~1 ps in hexane but ~12.5 ps in ethylene glycol (EG). This important finding enables a conclusion that the excited-state species having a double-bond character, i.e., the S_1 state with a planar structure, is generated following S_2 excitation. It questioned the dual mechanism in which the rotational isomerization proceeds directly from the S_2 state. Fujino et al.[13,21] measured the fluorescence dynamics of AB at $\lambda_{ex} = 280$ nm; the transients observed in a wide fluorescence wavelength region ($\lambda_{fl} = 340-680$ nm) show clearly two components that were attributed to the S_2 and S_1 fluorescence. These workers analyzed the lifetimes to be ~100 fs and ~500 fs for the rapid and slow components, respectively; the quantum yield for $S_2 \rightarrow S_1$ fluorescence was determined to be 1.07, indicating that the isomerization takes place after relaxation to the S_1 state. Since the isomerization in the S_1 state was considered to take place with inversion as proposed by Rau and Lüddecke,[10] they concluded that the isomerization of *trans*-azobenzene occurs with inversion regardless of difference in the initial excitation. As this mechanism seems to disagree with the hypothesis of Rau and Lüddecke[10] to rationalize the discrepancy of trans → cis isomerization yields between S_1 and S_2 excitations, Fujino et al.[13,21] proposed another relaxation channel to be open only for *trans*-$S_1 \rightarrow$ *trans*-S_0 in a vibrationally hot S_1 state.

Other time-resolved spectral investigations provide insights into this controversial mechanism of photoisomerization of AB and its derivatives. On excitation at 330 nm, Schultz et al.[23] found two distinct transient components using femtosecond time-resolved photoelectron spectroscopy with a molecular beam. Two electronic states, S_2 and $S_{3,4}$, were consequently proposed to be involved in the observed bifurcated relaxation dynamics: the S_2 population decays in 170 fs via the inversion channel to produce both cis and trans isomers, whereas the $S_{3,4}$ population decays in 420 fs via an uncharacterized channel to produce only the trans isomer on the ground-state PES. In this way, the proposed mechanism becomes consistent with both results on quantum yield[9] and observations of Tahara and coworkers.[13,20,21]

Working with AB derivatives, Saito and Kobayashi[38] discovered coherent modulations corresponding to NN- and CN-stretching modes of methyl yellow in dimethyl sulfoxide using a sub-10-fs chirp-controlled pump−probe technique. The authors claimed a multidimensional property of the excited-state surface such that a one-dimensional model via rotation or inversion is inadequate to describe the isomerization of AB derivatives. Sawada and co-workers[39,40] studied S_2 photoisomerization dynamics of methyl orange encapsulated in various cyclodextrin environments using an ultrafast transient lens technique; their results show that the rate of isomerization decreases, with a value of ϕ decreased from 0.1 to 0.07, when the molecule was completely confined in the nanospace. This observation is consistent with work of Bortolus and Monti,[34] who found quantum yields of photoisomerization of AB in a cyclodextrin cavity to be small, $\phi \approx 0.1$, and equal for both S_1 and S_2 excitations. With a synthetic strategy to impede rotation with a cyclophane structure[10] or a crown ether,[33] the quantum yields were, however, found to be larger, $\phi = 0.2-0.3$, but still equal for both electronic excitations.

Quantum-chemical characterization of potential-energy surfaces (PES) of excited states along inversion and rotation coordinates became practicable recently; previous work of Monti et al.[35] with minimal basis-set CI calculations rendered only a qualitative picture to describe the photochemistry of AB. Using advanced methods such as CASSCF and CIPSI with a larger basis set, Cattaneo and Persico[25] obtained excited-state potential-

(31) Zimmerman, G.; Chow, L.-Y.; Paik, U.-J. *J. Chem. Phys.* **1958**, *80*, 3528−3531.
(32) Bortolus, P.; Monti, S. *J. Phys. Chem.* **1979**, *83*, 648−652.
(33) Rau, H. *J. Photochem.* **1984**, *26*, 221−225.
(34) Bortolus, P.; Monti, S. *J. Phys. Chem.* **1987**, *91*, 5046−5050.
(35) Monti, S.; Orlandi, G.; Palmieri, P. *Chem. Phys.* **1982**, *71*, 87−99.
(36) Hirose, Y.; Yui, H.; Sawada, T. *J. Phys. Chem. A* **2002**, *106*, 3067−3071.
(37) Mayer, S. G.; Thomsen, C. L.; Philpott, M. P.; Reid, P. J. *Chem. Phys. Lett.* **1999**, *314*, 246−254.
(38) Saito, T.; Kobayashi, T. *J. Phys. Chem. A* **2002**, *106*, 9436−9441.
(39) Takei, M.; Yui, H.; Hirose, Y.; Sawada, T. *J. Phys. Chem. A* **2001**, *105*, 11395−11399.
(40) Yui, H.; Takei, M.; Hirose, Y.; Sawada, T. *Rev. Sci. Instrum.* **2003**, *74*, 907−909.

energy curves of AB that differ significantly in many aspects from those of Monti et al.[35] Ishikawa et al.[26] performed two-dimensional surface-scan calculations for S_0, $S_1(n,\pi^*)$, $S_2(\pi,\pi^*)$, and $S_3(n^2,\pi^{*2})$ states of AB using high-level CASSCF and MRCISD methods; Diau[15] performed CASSCF surface-scan calculations along the minimum energy pathway of several key reaction coordinates (RC) on the S_1 surface; Fliegl et al.[27] predicted vibrational and electronic spectra of AB using the coupled-cluster model; Cembran et al.[29] characterized lowest singlet and triplet excited-state PES along the rotational RC based on the CASPT2 approach. The gist of results from sophisticated methods indicates that the S_1 PES of AB involves a substantial energy barrier along the inversion coordinate, but has essentially no barrier along the rotational RC. Furthermore, the results of Ishikawa et al.,[26] Cembran et al.,[29] and Diau[15] show that a conical intersection (CI) between the S_0 and the S_1 states is located near the midpoint of the rotational pathway, indicating that photoisomerization of AB on the S_1 surface might favor the rotation mechanism. Persico and co-workers[14] simulated the dynamics of AB flying on both S_1 and S_2 surfaces using a semiclassical surface-hoping approach; their results indicate that the rotation channel is the preferred mechanism for photoisomerization of AB regardless of initial excitation. In view of the coherence of these theoretical calculations, key experimental evidence is required to resolve the inversion−rotation controversy about the mechanism.

As time-resolved fluorescence spectroscopy bestows an advantage of a well-defined detection window between the target excited state and the ground state, it might provide important dynamical information to enhance understanding of the photochemistry of azobenzene from a fundamental point of view. Fluorescence experiments of Fujino et al.[13,21] provide crucial dynamical information on excitation to the S_2 state, but the mechanistic information on S_1 excitation was inferred. We reported[22] the fluorescence dynamics of *trans*-azobenzene in hexane on excitation directly into the S_1 state ($\lambda_{ex} = 432$ nm). The temporal profiles of fluorescence feature two components that we assigned to decay of a rapid component reflecting structural relaxation from the Franck−Condon (FC) region and to decay of a slow component arising from essential nuclear motions along the rotational coordinate in seeking the rotational conical intersection (S_0/S_1 CI_rot) on the multidimensional PES. In the present work, we verify the rotation mechanism by means of fs time-resolved measurements of fluorescence anisotropy at three excitation wavelengths, $\lambda_{ex} = 400$, 440, and 480 nm, in a broad range ($\lambda_{fl} = 520-680$ nm) of fluorescence wavelength; we found that the S_1 anisotropy dynamics of AB depend strongly on the viscosity of the solvent. The observed S_1 fluorescence depolarization of AB in a nonviscous solvent, e.g., hexane, is highly anisotropic with a decay parameter the same as that of the slow component of the fluorescence transients. This observation indicates an orientational change of the transition dipole moment induced via structural relaxation along the rotational pathway in seeking S_0/S_1 CI_rot on the S_1 PES. In contrast, the fluorescence anisotropy for AB in a viscous solvent, ethylene glycol, decays only slightly when rotational motion is substantially constrained. The observed depopulation of S_1 fluorescence in EG therefore reflects in-plane symmetric motions along the concerted inversion reaction pathway in seeking another conical intersection (S_0/S_1 CI_inv). This mechanism not only rationalizes results both on quantum yields[9,10,31−34] and from ultrafast measurements,[13,16−24] but also is fully consistent with refined calculations[15,25,26] of electronic structure and semiempirical simulations of dynamics.[14]

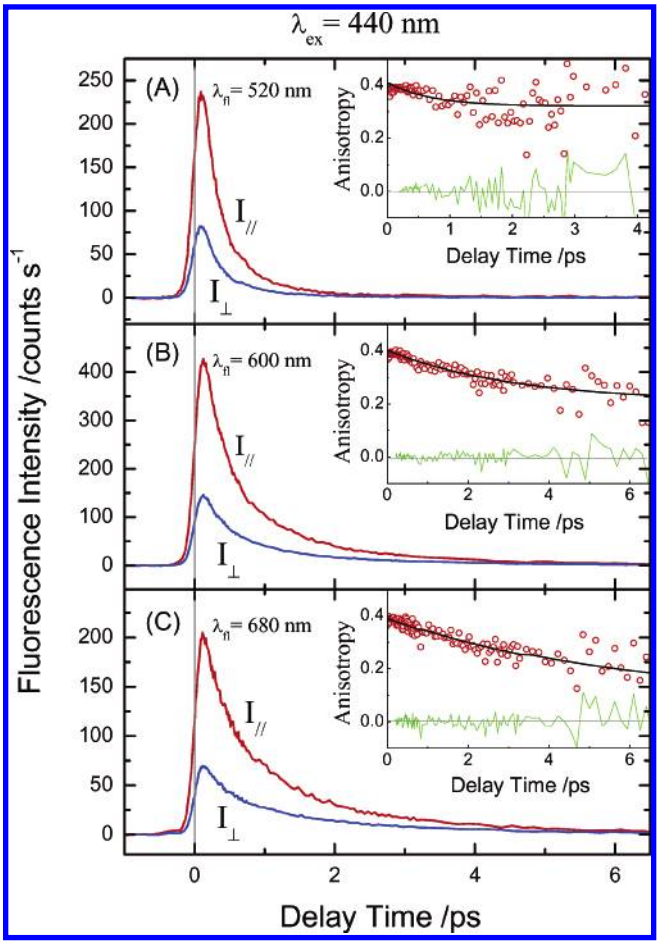

Figure 1. Polarized femtosecond fluorescence up-conversion transients of *trans*-azobenzene in hexane with excitation at $\lambda_{ex} = 440$ nm and detection at λ_{fl} = (A) 520 nm, (B) 600 nm, and (C) 680 nm with both parallel and perpendicular polarizations as indicated. Insets show the corresponding time-dependent fluorescence anisotropy data manipulated (shown as open circles) according to eq 1 and simulated (shown as solid curves) according to eq 4.

2. Results and Data Analysis

We performed time-resolved fluorescence anisotropy measurements using an integrated fluorescence up-conversion system in combination with a 76 MHz broadband (700−1000 nm) mode-locked Ti:sapphire laser of which the pulse duration was ~100 fs. A calibrated Berek's variable wave plate was used to vary the polarization of the excitation pulse with respect to the probe pulse. The experimental setup is detailed elsewhere,[22] and a summary is given in the Supporting Information. The experimental results and the subsequent kinetic analysis are presented in the following sections.

2.1. Evidence for Electronic Relaxation via the Rotation Channel. Figure 1 in three parts shows the fluorescence dynamics of *trans*-azobenzene in hexane with excitation wavelength fixed at $\lambda_{ex} = 440$ nm and emission observed at $\lambda_{fl} =$ 520, 600, and 680 nm. Time-dependent fluorescence anisotropy data shown in insets of these figures were obtained from manipulation of the corresponding fluorescence transients with

varied configurations of polarization between the pump and gate pulses according to the following formula:[41,42]

$$r(t) = \frac{I_{||}(t) - I_{\perp}(t)}{I_{||}(t) + 2I_{\perp}(t)} \quad (1)$$

in which $r(t)$ is the anisotropy at time t and $I_{||}(t)$ and $I_{\perp}(t)$ represent the time-dependent fluorescence intensities for the pump and gate pulses with parallel and perpendicular polarizations, respectively. $I_{||}(t)$ and $I_{\perp}(t)$ are formulated as follows:[42]

$$I_{||}(t) = \frac{I(t)}{3}[1 + 2r(t)] \quad (2)$$

$$I_{\perp}(t) = \frac{I(t)}{3}[1 - r(t)] \quad (3)$$

with the total intensity $I(t) = I_{||}(t) + 2I_{\perp}(t)$.

The observed data for time-dependent anisotropy exhibit three important features: the values of $r(t)$ at zero of delay time (r_0) are near 0.4, indicating the orientation of the dipole moments between excitation and emission to be nearly parallel at $t = 0$; $r(t)$ gradually decays, and a single-exponential decay function is applicable to describe this dynamical feature; $r(t)$ decays to a nonzero asymptotic level (r_∞) when both parallel and perpendicular fluorescence signals have reached nearly their background levels. Therefore, $r(t)$ is well-described according to the following equation:[41,42]

$$r(t) = (r_0 - r_\infty)\exp(-t/\tau_{rot}) + r_\infty \quad (4)$$

in which τ_{rot} is the time constant for rotational relaxation due to depolarization of the system. Before full analysis of the observed anisotropy dynamics, together with the corresponding time-resolved fluorescence data in a systematic way (see below), the time-dependent anisotropy data were initially fitted using only eq 4. From this preliminary analysis, both τ_{rot} and r_∞ were evaluated, depending on emission wavelength, to be in the ranges 1−3 ps and 0.2 to 0.3, respectively.

As detailed elsewhere for a general case,[42] the causes of the fluorescence depolarization might be nonparallel transition moments for absorption and emission, energy transfer to another molecule with disparate orientation, Brownian motion, or torsional vibrations. The first two factors can be excluded because of the theoretical value (~0.4) for r_0 observed and the simplicity of the system. Brownian rotation of the emission transition moment is also unlikely in the case for our observations in AB for two reasons: the observed single-exponential decay of the anisotropy has a decay time constant on a picosecond time scale (~2 ps), which is certainly too small for a rotational diffusion motion of a molecule such as AB to occur in a liquid state;[43] the observed anisotropy decays to an asymptotic level much above zero (r_∞ = 0.2−0.3), and this anisotropic feature seems inconsistent with motion of a free rotational type in solution for which $r_\infty = 0$. Therefore, a torsional vibration, presumably the CNNC-torsional motion, is responsible for the observed depolarization dynamics of AB in hexane. This experimental evidence is fully consistent with recent theoretical calculations.[14,15,25,26,29]

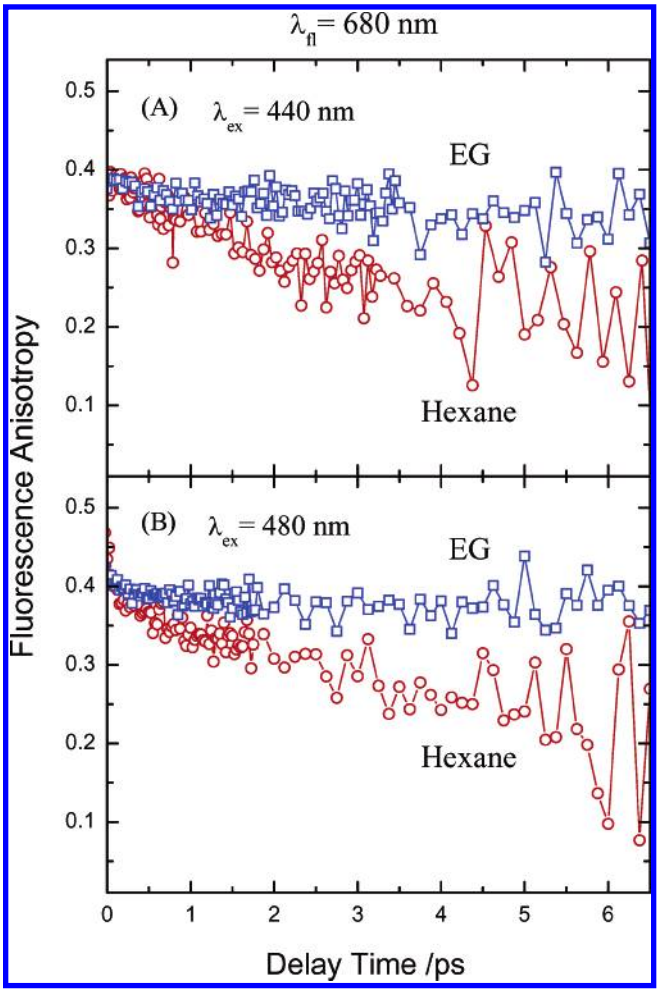

Figure 2. Comparison of time-dependent fluorescence anisotropy of *trans*-azobenzene in hexane (○) with anisotropy in ethylene glycol (□) probing at λ_{fl} = 680 nm with excitation at λ_{ex} = (A) 440 nm and (B) 480 nm.

If the CNNC-torsional motion is involved for the observed depolarization, this large-amplitude motion should be significantly hindered in a viscous solvent, ethylene glycol. In fact, we observed the decay of fluorescence anisotropy being much slower in EG than in hexane; the results appear in Figure 2A and B for λ_{ex} = 440 and 480 nm, respectively. To account quantitatively for these observations described above, we present a kinetic model.

2.2. A Kinetic Model for the Observed S_1 Dynamics. The observed anisotropy of *trans*-azobenzene in EG exhibits no discernible decay feature, whereas the corresponding fluorescence decays in a way that differs greatly from the decay of anisotropy (Figure 3). This distinction indicates another relaxation process that is insensitive to the depolarization of the system. The S_1 fluorescence depopulation might hence involve two relaxation channels: one corresponding to the out-of-plane CNNC-torsional motion that yields the observed S_1 depolarization dynamics and another related to a symmetric vibration (discussed later) without affecting the S_1 depolarization dynamics. As a result, the observed fluorescence intensity at parallel [$I_{||}(t)^{obsd}$] and perpendicular [$I_{\perp}(t)^{obsd}$] polarizations must be

(41) Lakowicz, J. R. *Principles of Fluorescence Spectroscopy*, 2nd ed.; Kluwer Academic/Plenum: New York, 1999; Chapters 10−12 and other related references therein.
(42) Valeur, B. *Molecular Fluorescence*; Wiley-VCH: Weinheim, Germany, 2002; Chapters 5 and 6 and other related references therein.
(43) Toele, P.; Zhang, H.; Glasbeek, M. *J. Phys. Chem. A* **2002**, *106*, 3651−3658.

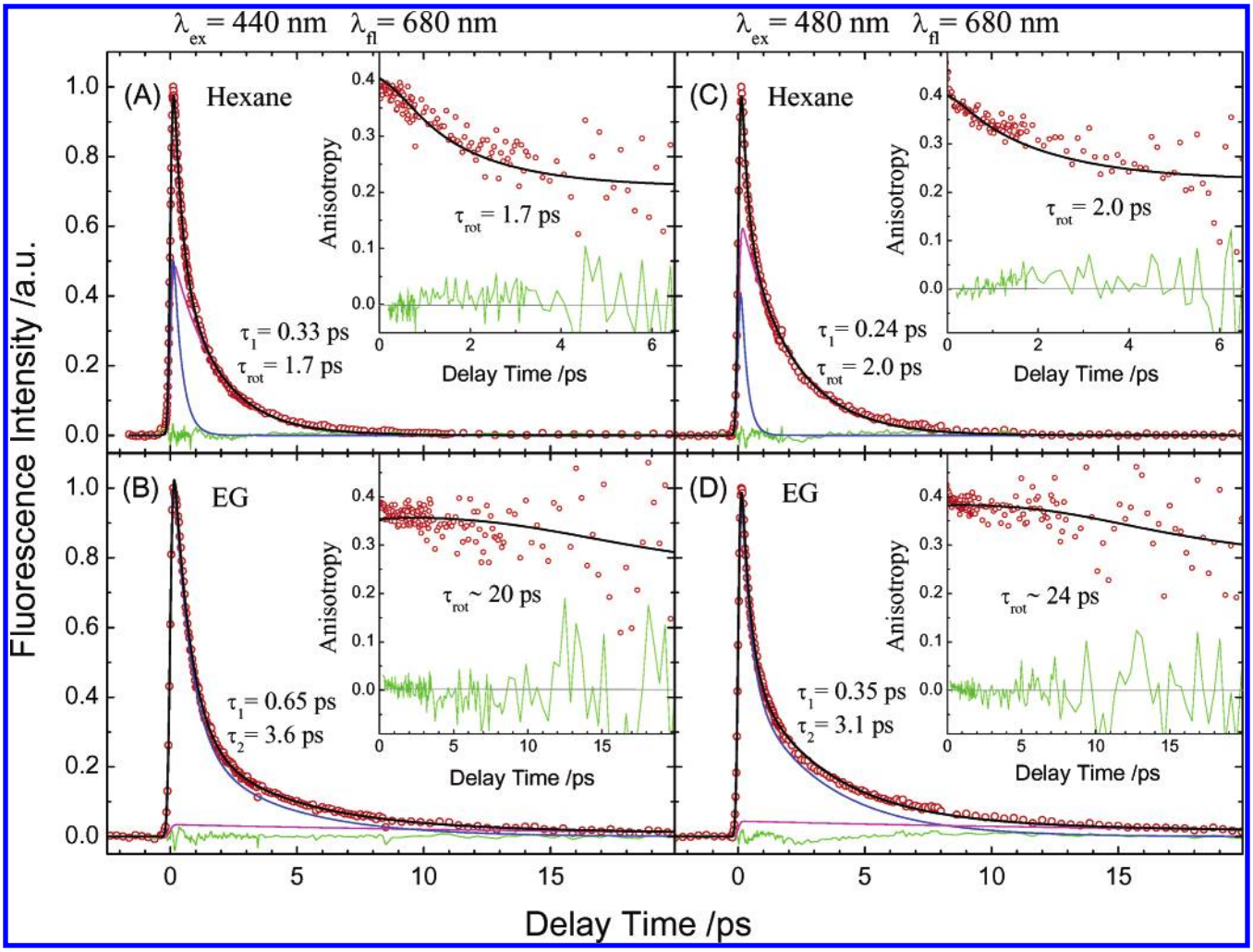

Figure 3. Normalized total time-dependent fluorescence intensity $I_{tot}(t)$ of *trans*-azobenzene with $\lambda_{ex} = 440$ nm and $\lambda_{fl} = 680$ nm in (A) hexane and (B) ethylene glycol, and $I_{tot}(t)$ with $\lambda_{ex} = 480$ nm and $\lambda_{fl} = 680$ nm in (C) hexane and (D) ethylene glycol. $I_{tot}(t)$ and the corresponding time-dependent fluorescence anisotropy data (shown in insets) were simultaneously analyzed according to eqs 5−13. The solid black curves are theoretical fits with residues shown as green traces; the red and blue curves under each transient are the deconvoluted components corresponding to $I_{rot}(t)$ and $I_{sym}(t)$, respectively.

modified according to eqs 2 and 3, respectively, to include contributions originating in both relaxation channels:

$$I_{\parallel}(t)^{obsd} = \frac{I_{rot}(t)}{3}[1 + 2r_{rot}(t)] + \frac{I_{sym}(t)}{3}[1 + 2r_{sym}] \quad (5)$$

$$I_{\perp}(t)^{obsd} = \frac{I_{rot}(t)}{3}[1 - r_{rot}(t)] + \frac{I_{sym}(t)}{3}[1 - r_{sym}] \quad (6)$$

in which $I_{rot}(t)$ and $I_{sym}(t)$ are the time-dependent fluorescence intensities resulting from rotational and symmetric vibrational channels, respectively; $r_{rot}(t)$ is the time-dependent anisotropy that decays as a function of time via the rotational relaxation channel, whereas r_{sym} is the time-independent anisotropy that does not decay via the symmetric vibrational relaxation channel. Similarly, $r_{rot}(t)$ is formulated according to eq 4:

$$r_{rot}(t) = (r_0 - r_\infty)\exp(-t/\tau_{rot}) + r_\infty \quad (7)$$

The time-dependent total fluorescence intensity $[I_{tot}(t)]$ is a sum of the time-dependent intensities of the individual channels:

$$I_{tot}(t) = I_{rot}(t) + I_{sym}(t) = I_{\parallel}(t)^{obsd} + 2I_{\perp}(t)^{obsd} \quad (8)$$

The observed time-dependent anisotropy, $r(t)^{obsd}$, becomes modified based on eqs 5−8, accordingly:

$$r(t)^{obsd} = \frac{I_{\parallel}(t)^{obsd} - I_{\perp}(t)^{obsd}}{I_{tot}(t)} = \frac{I_{rot}(t)}{I_{tot}(t)} r_{rot}(t) + \frac{I_{sym}(t)}{I_{tot}(t)} r_{sym} \quad (9)$$

The physical meaning of eq 9 is obvious: the anisotropy component resulting from the rotational relaxation channel decays exponentially as expressed in eq 7, whereas the other component resulting from the symmetric vibrational relaxation channel does not decay in time. The observed time-dependent anisotropy is a sum of these two components weighted by their corresponding intensities. Accordingly, we expect to detect an apparent anisotropy decay if the contribution from the rotational channel is dominant as in the case of hexane, whereas no apparent anisotropy decay is expected if the contribution from the symmetric vibrational channel prevails, as in the case of EG.

Figure 3, parts A and B, shows time-dependent total fluorescence intensity data (circles) according to eq 8 with $\lambda_{ex} = 440$ nm and $\lambda_{fl} = 680$ nm in hexane and EG, respectively; the corresponding time-dependent anisotropy data (circles)

Table 1. Summary of the Fitted Time Constants and the Corresponding Anisotropy Parameters at Various Excitation and Fluorescence Wavelengths[a]

solvents	λ_{ex}/nm	λ_{fl}/nm	FWHM[b]/fs	τ_1/fs	τ_2/ps	τ_{rot}/ps	r_0	r_∞	r_{sym}[c]
hexane	400	600	230	230 (0.74)		1.5 (0.26)	0.39	0.24	0.39
	440	520	220	150 (0.76)		0.6 (0.24)	0.41	0.32	0.41
		600	200	290 (0.69)		1.4 (0.31)	0.41	0.26	0.41
		680	190	330 (0.59)		1.7 (0.41)	0.40	0.21	0.40
	480	600	210	120 (0.70)		1.3 (0.030)	0.40	0.25	0.40
		680	180	240 (0.51)		2.0 (0.49)	0.40	0.22	0.40
ethylene glycol	440	680	210	650 (0.75)	3.6 (0.22)	20 (~0.026)	0.40[d]	0.21[d]	0.35
	480	680	180	350 (0.62)	3.1 (0.35)	24 (~0.034)	0.40[d]	0.22[d]	0.38

[a] Relative weights are given in brackets; the systematic ascending variation of τ_1 and τ_{rot} as a function of λ_{fl} is due to the detection window that is broader at greater wavelengths but narrower at smaller wavelengths.[22] [b] Values are the full width at half maximum of the instrument response function obtained from the fit; the systematic variation of the values as a function of λ_{fl} is due to the effect of group velocity dispersion (GVD) detailed elsewhere.[22] [c] Assume $r_{sym} = r_0$ in hexane but set r_{sym} as a free parameters in ethylene glycol (see text). [d] Values were fixed according to the case in hexane at the same λ_{ex} and λ_{fl}.

according to eq 9 are shown in insets. Figure 3, parts C and D, shows corresponding results obtained with $\lambda_{ex} = 480$ nm and $\lambda_{fl} = 680$ nm in hexane and EG, respectively. To describe $I_{tot}(t)$ properly, the transient signals were fitted with a convolution of the instrument response function with the molecular response function:[42,44]

$$I_{tot}(t) = I_{rot}(t) + I_{sym}(t) = \int_{-\infty}^{t} g(s)[f_{rot}(t-s) + f_{sym}(t-s)]\,ds \quad (10)$$

in which $g(s)$ is a Gaussian function; $f_{rot}(t)$ and $f_{sym}(t)$ are the molecular response functions for $I_{rot}(t)$ and $I_{sym}(t)$, respectively. Because the time-dependent anisotropy in hexane shows only a single-exponential feature with kinetics similar to the corresponding transient, the molecular response function, $f_{rot}(t)$, due to relaxation through the rotational channel becomes well-represented with a single-exponential function and a decay time constant equal to τ_{rot}:

$$f_{rot}(t) = a \exp\left(-\frac{t}{\tau_{rot}}\right) \quad (11)$$

The molecular response function, $f_{sym}(t)$, due to relaxation through the symmetric vibrational channel is also represented with a single-exponential function and a decay time constant (τ_1):

$$f_{sym}(t) = a_1 \exp\left(-\frac{t}{\tau_1}\right) \quad (12)$$

Figures 2 and 3 clearly show that the motion through the rotational channel in EG slows significantly, so that relaxation contributed from the symmetric vibrational channel becomes important. As the single-exponential molecular response function, eq 12, is inadequate to fit $I_{tot}(t)$ in EG, we obtained the theoretical curves shown in Figure 3B and D using a biexponential function with decay time constants τ_1 and τ_2 representing rapid and slow decays, respectively:

$$f'_{sym}(t) = a_1 \exp\left(-\frac{t}{\tau_1}\right) + a_2 \exp\left(-\frac{t}{\tau_2}\right) \quad (13)$$

According to this analysis, data for both time-dependent fluorescence, $I_{tot}(t)$, and anisotropy, $r(t)^{obsd}$, shown in Figure 3, were simultaneously fitted according to eqs 5−13; the fitted results are shown as solid curves. Data in eight sets (see Supporting Information) were satisfactorily fitted with this kinetic model; the results are summarized in Table 1.

3. Discussion

Our observations in real time can be summarized according to the following three major points. First, there are two genuine dynamical processes involved in the observed S_1 fluorescence decays in hexane, but only a single exponential decay was observed in the corresponding anisotropy decays, with kinetics identical to the slow decay component of the transients. Second, when the rotational motion was substantially restricted in a viscous solvent, for example, ethylene glycol, the fluorescence anisotropy seems not to decay in time, and the S_1 fluorescence dynamics must be described by at least three dynamical processes; the dominant relaxation via the symmetric vibrational channel is biphasic in nature. Third, the fitted decay time constants in hexane depend systematically on the fluorescence wavelength,[22] but their dependence on excitation energy has an atypical trend. These dynamical behaviors can be understood to some extent with the aid of theoretical calculations, discussed in what follows.

3.1. A Relaxation Mechanism for the Observed S_1 Dynamics. Rotational relaxation in hexane has been unambiguously observed (Figure 3A and C) with a relaxation time constant (τ_{rot}) evaluated in a range 0.6−2.0 ps (Table 1) depending on the fluorescence wavelength.[22] The observed rates of decay, τ_{rot}^{-1}, in EG are about one tenth of those in hexane (Table 1); this disparity is understood to reflect that nuclear motion through the rotation channel is substantially hindered and slowed in the viscous solvent. The transients in EG (Figure 3B and D) show an offset-like component for a slow decay, $\tau_{rot} \approx 20$ ps, with only a slight contribution, ~0.03, corresponding to the slow rotational motion, whereas the transients in hexane decay rapidly to the background level in 10 ps (Figure 3A and C). Our results thus indicate that the relaxation $S_1 \rightarrow S_0$ through the rotation channel is dominant in hexane but scarcely observed in EG.

Excited-state calculations[15] indicate two possible isomerization channels to lead to the photochemical funnels responsible for the observed S_1 dynamics. One follows the rotation—the out-of-plane CNNC-torsional motion—pathway on an almost flat S_1 surface, at which a conical intersection (S_0/S_1 CI_rot) is accessible at a molecular structure with the CNNC-torsional angle near a perpendicularly twisted conformation. The other follows the concerted inversion—the in-plane symmetric CNN-bending motion—pathway descending to approach a planar

(44) Pedersen S.; Zewail, A. H. *Mol. Phys.* **1996**, *89*, 1455−1502.

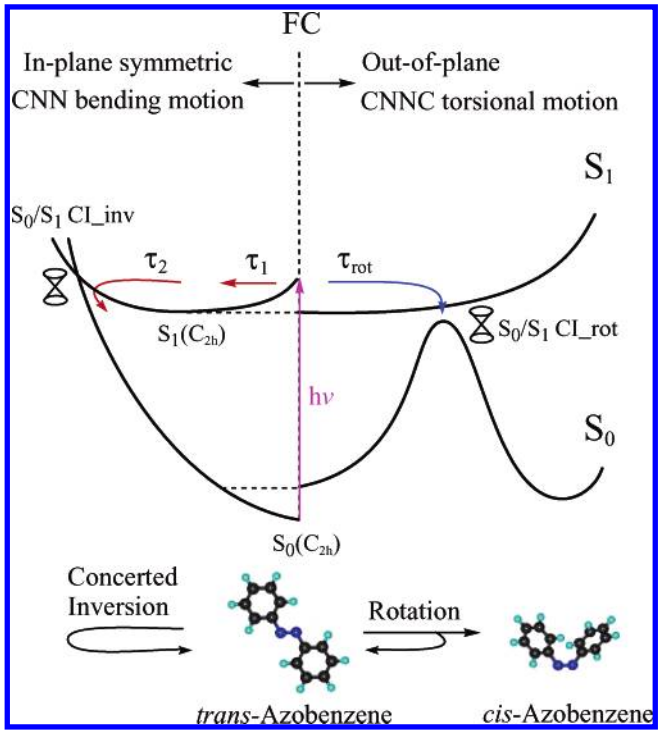

Figure 4. A dynamical representation based on theoretical calculations[15] to illustrate two relevant reaction channels responsible for the observed dynamics of photoisomerization of *trans*-azobenzene on the S_1 potential-energy surface in various solvents.

region of local minimum at the $S_1(C_{2h})$ geometry; following this reaction path might lead to a sloped conical intersection (S_0/S_1 CI_inv) at the molecular structure near a linear CNNC conformation. On the basis of these theoretical findings, a dynamical picture is displayed in Figure 4 to illustrate the observed dynamics of photoisomerization of AB on the S_1 PES. Our observations support the above dynamical picture: the observed rate of S_1 depolarization, τ_{rot}^{-1}, in hexane is due to electronic relaxation through the rotation channel via S_0/S_1 CI_rot, whereas the observed rate of S_1 fluorescence depopulation, τ_2^{-1}, in EG is consistent with relaxation mainly due to the concerted inversion channel via S_0/S_1 CI_inv.

3.2. An Intensity-Borrowing Mechanism upon Initial S_1 Excitation. In the following, we present a possible dynamical model based on the intensity-borrowing mechanism of a symmetry-forbidden transition to rationalize the observed depolarization dynamics of *trans*-azobenzene in hexane. As the molecule in its ground electronic state belongs to point group C_{2h}, the $S_0(A_g) \rightarrow S_1(B_g)$ transition is strictly forbidden by symmetry. For this forbidden $n\pi^*$ transition to occur, the intensity might be "borrowed" from an upper symmetry-allowed transition through an appropriate vibronic coupling process.[45] Refined calculations[14,23,25−27] of molecular electronic structure indicate that the next transition, of type $\pi-\pi^*$ that is allowed by symmetry, occurs to an electronic state with B_u symmetry. If this B_u state is borrowed from accordingly, the dipole moment for the electronic transition would have B_u symmetry because the representation character of the electronic transition dipole moment matrix element $\langle A_g|\mu|B_u\rangle$ is totally symmetric. As a result, the transition dipole moment of the molecule at time zero ($\hat{\mu}_0$) is polarized inside the *xy*-plane for a nonzero absorption intensity being observed. For the case of *trans*-azomethane, an azo compound also having C_{2h} symmetry, work on photodissociation in the gaseous phase[46,47] indicated that $\hat{\mu}_0$ is oriented parallel to the NN double bond of the azo group; the case of *trans*-azobenzene might be also similar. On the basis of a first-order approximation, the intensity borrowed from the next symmetry-allowed state with B_u symmetry would require the symmetry of the corresponding vibrational motion (Q) to satisfy the totally symmetric criterion for the matrix element $\langle B_g|Q|B_u\rangle$. Therefore, Q would correspond to a vibrational motion with A_u symmetry for absorption intensity borrowed from an upper B_u state. In principle, all normal-mode vibrations with A_u symmetry belong to motion of an out-of-plane type; the CNNC-torsional mode is considered for the observed S_1 depolarization in hexane because of the following two reasons.

First, the rotational relaxation time constant of the anisotropy decay (τ_{rot}) is identical to the time constant for fluorescence decay of the slow component of the transients, meaning that the depolarization of the system reflects the electronic relaxation via the rotation channel as discussed in section 3.1. Second, the observed anisotropy decays to a nonzero asymptotic level (r_∞) related to the detection window of the fluorescence probe. The data shown in Figure 1 indicate that at $\lambda_{ex} = 440$ nm, a larger r_∞ value was observed at the smaller emission wavelength ($r_\infty \approx 0.3$ at $\lambda_{fl} = 520$ nm), whereas a smaller r_∞ value was obtained at a larger emission wavelength ($r_\infty \approx 0.2$ at $\lambda_{fl} = 680$ nm) because the detection window is broader for the latter.[22] A broader detection window would probe the CNNC-torsional motion more extensively, which is expected to lead to a larger angular displacement being observed.

3.3. Initial Driving Force Affecting the Rapid S_1 Dynamics. In EG, a biexponential decay function, eq 13, served to fit properly the time-dependent fluorescence signals for the S_1 species relaxing through the concerted inversion channel. This biphasic dynamical nature implies that there must be an initial process with time constant τ_1 for nuclear relaxation from the FC region to the local minimum area on the S_1 PES. This FC relaxation, as proposed previously,[22] is insensitive to the fluorescence depolarization, a phenomenon that we have also observed in hexane, with time constant τ_1. The observed initial fluorescence decay in both EG and hexane is hence related to a symmetrical nuclear motion, in-plane vibration, that does not depolarize $\hat{\mu}_0$. The feasible in-plane symmetric vibrations are the symmetric CNN-bending motion, the symmetric CN-stretching motion, and the NN-stretching motion. According to theoretical calculations,[15] the structure of the local minimum [$S_1(C_{2h})$] has a CNN-bending angle somewhat larger than the angle at the FC geometry (128.7° vs 116.8°); the CN bond of the $S_1(C_{2h})$ species is also shorter than that of the FC structure (1.384 Å vs 1.428 Å). Moving from the FC region along either the symmetric CNN-bending RC or the symmetric CN-stretching RC directions to the $S_1(C_{2h})$ area would gain substantial internal energy; this energetic factor might be the driving force for what we have observed in the initial stage upon excitation to the $S_1(n,\pi^*)$ state. The horizontal dotted lines shown in Figure

(45) Herzberg, G. *Molecular Spectra and Molecular Structure III. Electronic Spectra and Electronic Structure of Polyatomic Molecule*, Van Nostrand Reinhold: New York, 1967; p 137 and other related references therein.
(46) Gejo, T.; Felder, P.; Huber, J. R. *Chem. Phys.* **1995**, *195*, 423−433.
(47) Diau, E. W.-G.; Zewail, A. H. *Chem. Phys. Chem.* **2003**, *4*, 445−456 and references therein.

4 further emphasize this point. The calculated relative energy of the $S_1(C_{2h})$ species is less than the energy at the FC structure by 12.3 kcal mol^{-1} but is only slightly greater than for the S_1 true minimum (C_2 symmetry) by 1.0 kcal mol^{-1}.[15]

The observed rate of rapid decay, τ_1^{-1}, depends on energy; it is greater with less excitation energy at 480 nm but smaller with more energy at 440 nm in both hexane and EG (Table 1). This opposite trend can be rationalized for a vibronic coupling effect through in-plane symmetric motions being stronger at 480 nm than at 440 nm. As noted previously, the symmetric CNN-bending motion and the symmetric CN-stretching motion effectively bring the S_1 potential energy down to the level near the $S_1(C_{2h})$ local minimum energy. The FC structure for 480-nm excitation is therefore expected to have a geometry nearer that of the $S_1(C_{2h})$ species than of the FC structure with excitation at 440 nm; the vibronic interaction involving in-plane symmetric vibrations is expected also to be stronger for the former than for the latter. As a result, the driving force upon initial excitation is vibronic coupling through symmetrical in-plane vibrations; this driving force is much stronger with excitation at 480 nm than the driving force at 440 nm. The rate of decay, τ_1^{-1}, observed at 400 nm with greater excitation energy is nevertheless greater than the rate of decay observed at 440 nm with smaller excitation energy. This normal dynamical phenomenon probably involves redistribution of intramolecular vibrational energy (IVR) when the vibronic coupling effect becomes less important at $\lambda_{ex} = 400$ nm.

3.4. Vibronic Coupling Affecting the Slow S_1 Dynamics. In hexane, the rotational motion is active and becomes a major $S_1 \rightarrow S_0$ relaxation channel. Except for relaxation through the rotation channel, only a single-exponential decay, described by eq 12, corresponding to the initial FC relaxation was observed. We have tried to fit our transients also using eqs 10, 11, and 13 for a possible contribution of the concerted inversion channel in hexane. In an extreme case with τ_1 fixed at 50 fs, the smallest time constant resolvable with our instrument, τ_2 was obtained in a range 0.3−0.6 ps. The relaxation times through the concerted inversion channel ($\tau_2 = 0.3-0.6$ ps in the higher limit) are still much smaller than those through the rotation channel ($\tau_{rot} = 0.6-2.0$ ps; Table 1), which is inconsistent with our observation that the latter is a major relaxation channel. The contribution to $S_1 \rightarrow S_0$ relaxation from the concerted inversion channel is thus expected to be negligible in hexane.

The above discussion implies that the concerted inversion channel is open only when the rotation channel is blocked. From a dynamical point of view, the sloped nature of the S_0/S_1 CI_inv (Figure 4) indicates vibronic coupling to be involved for efficient internal conversion. According to discussion in section 3.3, the most effective vibronic coupling upon initial excitation is through the symmetric CNN-bending motion. The effect of vibronic interaction with this in-plane vibration might be significant only at a structure near a planar conformation. Once the molecule moves along the rotational pathway to a certain extent as in the case of hexane, the effect of vibronic interaction might become insignificant, leaving the only channel for electronic relaxation to be rotation. If rotational motion is suppressed as in EG, vibronic coupling via the symmetric CNN-bending motion is expected to be efficient so that internal conversion through the concerted inversion channel occurs on the observed picosecond time scale; an excitation with less internal energy (i.e., $\tau_2 = 3.1$ ps at 480 nm but $\tau_2 = 3.6$ ps at 440 nm) facilitates this process.

3.5. Subtle Evidence for Initial Asymmetric Motions in Ethylene Glycol. Saito and Kobayashi[38] observed strong dynamical mode coupling between the NN- and CN-stretching modes before isomerization through torsional motion in the system of methyl yellow, which indicates the multidimensionality of the potential surfaces relevant to the reaction in the excited state. We have additional information about the observed S_1 depolarization dynamics of AB in EG to provide a multidimensional feature of the S_1 PES that Saito and Kobayashi have noted. In Table 1 the fitted r_{sym} values in EG, 0.35 and 0.38, are smaller than those in hexane, 0.39−0.41. In Figure 2 there is a subtle early-time anisotropy decay feature not being considered for the time-independent anisotropy parameter, r_{sym}, in eq 9; for this reason we observed smaller r_{sym} values in EG. To account for such a subtle difference in the observed S_1 anisotropy dynamics, we must allow r_{sym} to relax from an initial value, r'_0, to an asymptotic level, r'_∞, with a time constant τ' similar to the case of $r_{rot}(t)$ in eq 7:

$$r_{sym}(t) = (r'_0 - r'_\infty)\exp(-t/\tau') + r'_\infty \qquad (14)$$

By replacing r_{sym} with $r_{sym}(t)$ in eq 9, we fit both transient and anisotropy data perfectly according to the same kinetic model mentioned above. The new results show values of r'_0 to be 0.39 and 0.40 and values of r'_∞ to be 0.34 and 0.37 with $\lambda_{ex} = 440$ and 480 nm, respectively, with $\tau' \approx 1$ ps in both cases; according to this modified kinetic model the other time constants and the relative weights were evaluated to be the same as before.

Figure 5, parts A and B, demonstrates the subtle difference of $r(t)^{obsd}$ between the two models at $\lambda_{ex} = 440$ and 480 nm, respectively; the fluorescence transients were fitted to be identical to cases shown in Figure 3B and D. Although the change in anisotropy is minute and even smaller than the noise at larger times, the decay feature is clearly visible in the insets of Figure 5 at small times when the noise is modest. This small but significant evidence indicates another dynamical process to be involved at an early stage with a relaxation time of order 1 ps. As the quality of data is inferior to represent such a small variation in anisotropy, we obtained only approximate τ' values from the fit. The fit of $I_{tot}(t)$ in Figure 3D is imperfect, which might indicate an involvement of another decay component (unresolvable from the fit because of its small contribution) generating the observed depolarization. We consider this subtle initial depolarization in EG to be due to certain asymmetric motions that alter the transition dipole moment in early stages of reaction. The best candidate for the observed asymmetric motion is a coupled vibration between NN- and CN-stretching modes that Saito and Kobayashi[38] observed in the AB derivative. To account for our observation, an asymmetric in-plane CNN-bending motion might also depolarize the system. The contribution of the asymmetric motions is too small to be evaluated in the fit of transients in EG, and evidence is lacking for the involvement of this motion in hexane. The observed subtle decay in anisotropy might provide evidence for involvement of asymmetric motions, but they should be regarded only as part of the FC relaxation upon initial excitation.

3.6. Rationalization of the Inversion−Rotation Controversy. The dual mechanism for the photoisomerization of azobenezene (Scheme 1) has long been accepted on the basis

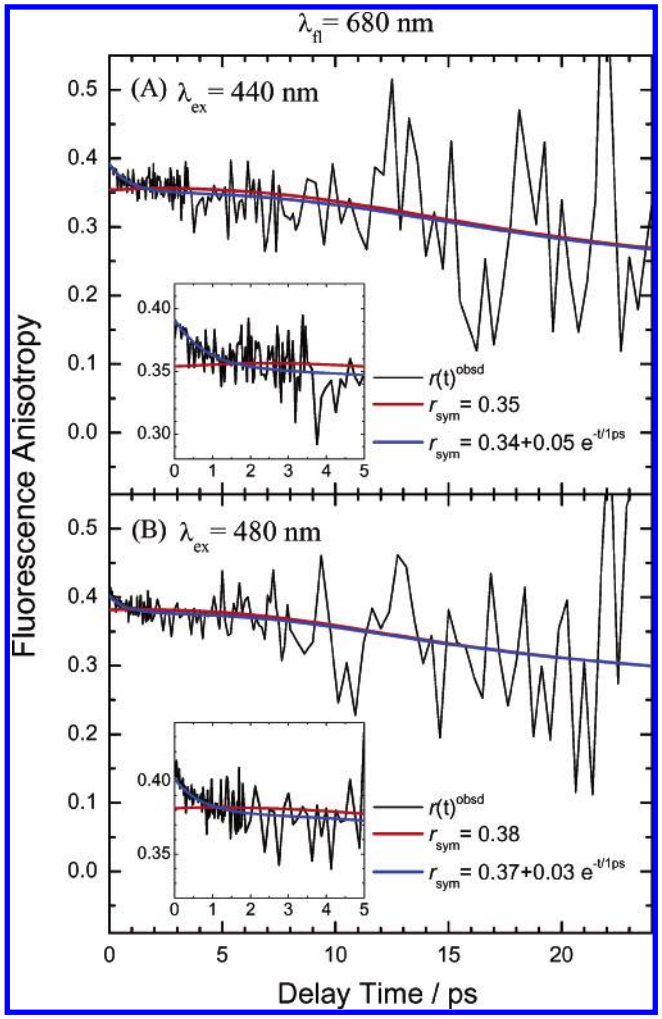

Figure 5. Time-dependent anisotropy in ethylene glycol (black traces) reanalyzed with the same kinetic model as in Figure 3B (A) and Figure 3D (B) but using $r_{sym}(t)$ instead of r_{sym}. The red and blue curves are theoretical fits obtained from old, r_{sym}, and new, $r_{sym}(t)$, models, respectively. The insets show a subtle decay feature that might be due to asymmetric motions responsible for part of the FC relaxation activated upon initial excitation (see text).

of measurements in a steady state.[9] The quantum yield for trans → cis isomerization depends on wavelength, $\phi \approx 0.25$ and $\phi \approx 0.1$ on S_1 and S_2 excitations, respectively, but it becomes essentially independent of wavelength ($\phi \approx 0.25$ on both excitations) when rotation about the NN double bond is restricted by chemical modifications.[9,10,33] Bortolus and Monti[34] evaluated ϕ to be smaller ($\phi \sim 0.1$ on both excitations) when the molecule was included in a confined nanospace (cyclodextrin); this important evidence should be taken into account in any conclusion. Our experimental results indicate that on S_1 excitation the $S_1 \rightarrow S_0$ relaxation through the rotation channel is dominant in hexane, whereas relaxation via the concerted inversion channel prevails in EG; in the latter case the inhibition of rotational motion in a viscous solvent might mimic a confined space. As isomerization via the rotation channel is expected to produce more cis isomer than that via the concerted inversion channel,[15] one thus expects to observe the quantum yield applicable to the rotation channel in hexane, $\phi \approx 0.25$, to be greater than the yield predominantly operating through the concerted inversion channel, $\phi \approx 0.1$, when the rotational motion becomes significantly hindered in the cyclodextrin nanocavity. This conclusion is supported also by femtosecond measurements of Sawada and co-workers,[39,40] who found the quantum yield of an AB derivative (methyl orange) in the confined space of cyclodextrins, $\phi \approx 0.07$ in a 1:2 complex, to be smaller than the yield in free aqueous solution, $\phi \approx 0.1$, on S_2 excitation with $\lambda_{ex} = 400$ nm.

Inconsistency of results for quantum yields between experiments on AB-cyclodextrin inclusion complexes, $\phi \approx 0.1$,[34,39,40] and the rotation-blocked AB derivatives, $\phi \approx 0.25$,[9,10,33] implies a subtle mechanistic discrepancy between these cases. As the rotation channel is blocked in both cases, only the concerted inversion pathway is feasible for trans → cis photoisomerization to occur. From a structural point of view, the two phenyl rings twist more easily about the two CN bonds in the former case than in the latter case for which structural restriction by other chemical bonds attached to the rings might be severe. According to the theoretical calculations,[15] this structural difference might have a significant dynamical effect by following the direction of the derivative coupling motion, corresponding to a symmetric out-of-plane CNN-bending vibration, of the conical intersection (S_0/S_1 CI_inv). Following this out-of-plane bending motion descending to the S_0 surface, the phenyl-ring-twisted S_0 species, with CNNC dihedral angle 180°, must revert the two phenyl rings to the same molecular plane for a stable trans isomer to be produced on the S_0 PES. As the twisting motion of the phenyl rings is suppressed in the case of rotation-blocked azobenzene derivatives, one expects that less *trans*-S_0 isomer, or more *cis*-S_0 isomer, becomes produced in this case than in the case of azobenzene−cyclodextrin inclusion complexes. The above speculation suggests the photoisomerization of AB and its derivatives to occur within the electronic *ground state* when the rotation channel is obstructed.

On excitation from the S_2 state ($\lambda_{ex} = 273$ nm), Fujino and Tahara[13,20] measured the picosecond Raman spectra of AB in both hexane and EG solvents. The most significant discovery made from the time-resolved Raman study is the fact that the transient Raman spectra corresponding to a planar species with NN double bond character were unambiguously observed in both solvents. Because this important finding did not give any support for the rotational mechanism,[13] it was suggested by the authors that the photoisomerization of AB on S_2 excitation takes place in the S_1 state by inversion.[20] The high similarity between the S_1 and the S_0 Raman spectra indicated that the observed S_1 species has a planar structure around the NN bond. However, this observation cannot exclude the following photoisomerization of AB to proceed through the rotation channel for the twisted S_1 species being either Raman inactive or extremely short-lived. There are two reasons to support this inference. First, the observed planar S_1 species in transient Raman spectra at time zero can only provide the evidence for an efficient $S_2 \rightarrow S_1$ internal conversion near its FC geometry, which has been confirmed by recent theoretical calculations[14] for the conical intersection (S_1/S_2 CI) being characterized to have nearly planar geometry. In fact, the ultrarapid nature of the $S_2 \rightarrow S_1$ relaxation process has been reported by recent transient absorption[13,18] and fluorescence up-conversion studies.[13,21] The assignment of the observed transient Raman spectra has also been made successful according to vibration wavenumbers of the planar $S_1(C_{2h})$

species calculated at the 14/12 CASSCF level.[48] Therefore, the structural information provided by time-resolved Raman study gives only the evidence for the $S_1(C_{2h})$ species being produced after the $S_2 \rightarrow S_1$ relaxation but gives no indication for the isomerization mechanism in the S_1 state.

Second, the lifetime of the observed planar S_1 species was found to be strongly solvent dependent, as short as ~1 ps in hexane (uncertain because of the limit of the time resolution of the instrument) but ~12.5 ps in EG.[13,20] The 1 order of magnitude discrepancy in lifetimes observed for the $S_1 \rightarrow S_0$ relaxation between the two solvents strongly suggests that two different isomerization pathways on the S_1 PES are involved on S_2 excitation. The transient Raman bands of AB in hexane disappeared in ~1 ps, which is consistent with our observation on direct S_1 excitation ($\tau_{rot} = 1-2$ ps; Table 1) for the rotation channel being dominant. However, the Raman bands in EG disappeared in a much longer time when the large-amplitude motions, such as the CNNC-torsional motion, are substantially hindered in the viscous solvent. The reported ~12.5 ps lifetime of AB in EG on S_2 excitation[13,20] is greater than what we observed in the same solvent on S_1 excitation ($\tau_2 = 3-4$ ps; Table 1). Disregarding the broader laser pulse (fwhm $\approx$ 2.8 ps) and the parallel pump−probe polarization used in the transient Raman experiments,[13,20] the discrepancy between the observed lifetimes might reflect a narrower detection window being probed in our case, as Satzger et al.[24] have noted, or some dynamical effect upon separate electronic excitations (S_2 vs S_1). Nevertheless, the observed τ_2 relaxation time obtained in EG in our work conforms with the femtosecond transient absorption result of Lednev et al.[19] (~2.6 ps) in a capped azobenzene for which the rotational motion is completely inhibited. In hexane, the observed rotational relaxation times ($\tau_{rot} = 0.6-2.0$ ps; Table 1) are slightly smaller than the S_1 lifetime (2.1−3.0 ps) observed in investigations of femtosecond transient absorption.[16−18,24] This discrepancy is understood on the basis of a narrower detection window of the fluorescence technique being employed than mentioned earlier.[22,24]

The decreased quantum yield on S_2 excitation[9] in hexane can be understood also to be due to involvement of the symmetric CNN-bending motion along the concerted inversion channel. Theoretical calculations[14] indicate that the key conical intersection (S_1/S_2 CI) on the trans side, $\angle$CNNC = 176°, has a smaller CNN-bending angle, 112°, than the angle at the FC structure, 117°. The subsequent trajectory simulations[14] indicate that the large amplitude of this symmetric CNN-bending motion leads to observation of an "early" $S_1 \rightarrow S_0$ internal conversion with larger CNNC-torsional angle for a smaller quantum yield being observed. The simulated results give $\phi = 0.33$ and 0.15 on S_1 and S_2 excitations, respectively. Although the values are slightly larger, the trend is consistent with that of steady-state measurements.[9] The observed bifurcated S_2 dynamics in isolated system[23] are rationalized, based on semiclassical simulations,[14] for one component corresponding to the S_2 (lifetime $\approx$ pulse-limited) $\rightarrow$ S_1 (lifetime = 420 fs) $\rightarrow$ S_0 process, which is consistent with the femtosecond fluorescence measurements in hexane on S_2 excitation;[13,21] the other component (lifetime = 170 fs) not being observed in solution might be due to the involvement of a twisted $n^2\pi^{*2}$ species characterized by the theoretical calculation.[48] In lack of considering the interaction with solvent molecules, the results obtained from simulation[14] of dynamics in the gaseous phase agree qualitatively with our observation in hexane that the rotation channel is the preferred mechanism for photoisomerization of azobenzene on S_1 excitation.

4. Conclusion

We addressed the controversy about the mechanism of photoisomerization of *trans*-azobenzene through direct observation of depolarization and depopulation dynamics of the molecule in solutions upon S_1 excitation by means of femtosecond fluorescence anisotropy. The observed prominent depolarization in hexane might be due to the variation of orientation of the transition dipole moment induced via structural relaxation along the CNNC-torsional pathway in seeking an efficient conical intersection (S_0/S_1 CI_rot) when the rotation channel is open in a nonviscous solvent. In contrast, the observed indiscernible anisotropy change in ethylene glycol is rationalized to be due to in-plane symmetric motions along the concerted inversion channel, corresponding to a symmetric CNN-bending vibration, to approach another conical intersection, S_0/S_1 CI_inv, for internal conversion when the rotational motion is obstructed in a viscous solvent. The proposed concerted inversion mechanism activated in ethylene glycol is consistent with results of transient Raman experiments by Tahara and co-workers[13,20] in which the planar S_1 intermediate was observed in the same solvent. We therefore propose that *the rotation channel is operative for the observed dynamics of photoisomerization of trans-azobenzene in a nonviscous solvent. When the rotation channel is obstructed in a viscous solvent, in inclusion complexes, or through chemical modification, the concerted inversion channel operates to account for the observed ultrafast electronic deactivation through this channel*. The results[9,10,31−34] for the quantum yield in a steady state and the femtosecond observations[13,16−24] are well-justified according to the proposed mechanism. The present experiments are fully supported by recent theoretical calculations[14,15,25,26,29,48] and may provide crucial dynamical information to resolve the mechanistic problem for an enduring classical controversy about the mechanism of photoisomerization of azobenzene.

Acknowledgment. We thank Prof. Maurizio Persico for many helpful discussions and his kindness in providing a manuscript before publication, and we thank Prof. Po-Yuan Cheng for many discussions. We are indebted to Prof. Tahara for his many insightful and stimulating discussions and invaluable suggestions. The suggestions made by Dr. John F. Ogilvie are much appreciated. The National Science Council of the Republic of China supported this work under project contract No. 92-2113-M-009-002.

Supporting Information Available: A summary for the experimental section, raw data in eight sets, and the subsequent averaged fluorescence/anisotropy data are given to supplement analyzed results summarized in Table 1. This material is available free of charge via the Internet at http://pubs.acs.org.

JA049215P

(48) Gagliardi, L.; Orlandi, G.; Bernardi, F.; Cembran A.; Garavelli, M. *Theor. Chim. Acc.* **2004**, *111*, 363−372.